TU Delft

Delft University of Technology

Scour Effect on the Lateral Bearing Behaviour of Monopiles Considering Different Slenderness Ratios

Li, Qiang; Wang, Xinquan; Gavin, Kenneth; Jiang, Shengxiang ; Diao, Hongguo ; Wang, Mingyuan; Wang, Kangyu

DOI
10.3390/w16020226

Publication date
2024

Document Version
Final published version

Published in
Water

Citation (APA)
Li, Q., Wang, X., Gavin, K., Jiang, S., Diao, H., Wang, M., & Wang, K. (2024). Scour Effect on the Lateral Bearing Behaviour of Monopiles Considering Different Slenderness Ratios. *Water*, *16*(2), Article 226. https://doi.org/10.3390/w16020226

Important note
To cite this publication, please use the final published version (if applicable).
Please check the document version above.

Copyright
Other than for strictly personal use, it is not permitted to download, forward or distribute the text or part of it, without the consent of the author(s) and/or copyright holder(s), unless the work is under an open content license such as Creative Commons.

Takedown policy
Please contact us and provide details if you believe this document breaches copyrights.
We will remove access to the work immediately and investigate your claim.

This work is downloaded from Delft University of Technology.
For technical reasons the number of authors shown on this cover page is limited to a maximum of 10.

water

MDPI

Article

Scour Effect on the Lateral Bearing Behaviour of Monopiles Considering Different Slenderness Ratios

Qiang Li [1,2], Xinquan Wang [1,3,4,*], Kenneth Gavin [5], Shengxiang Jiang [6], Hongguo Diao [1,3,4], Mingyuan Wang [6] and Kangyu Wang [7]

1 Department of Civil Engineering, Hangzhou City University, Hangzhou 310015, China; qiangli1991@outlook.com (Q.L.); diaohg@zucc.edu.cn (H.D.)
2 PowerChina Huadong Engineering (Shenzhen) Corporation Limited, Shenzhen 518100, China
3 Key Laboratory of Safe Construction and Intelligent Maintenance for Urban Shield Tunnels of Zhejiang Province, Hangzhou City University, Hangzhou 310015, China
4 Zhejiang Engineering Research Center of Intelligent Urban Infrastructure, Hangzhou City University, Hangzhou 310015, China
5 Faculty of Civil Engineering and Geosciences, Delft University of Technology, 2628 CN Delft, The Netherlands; k.g.gavin@tudelft.nl
6 PowerChina Huadong Engineering Corporation Limited, Hangzhou 310014, China; jiang_sx@hdec.com (S.J.); wang_my2@hdec.com (M.W.)
7 School of Civil Engineering, Zhejiang University of Technology, Hangzhou 310014, China; kangyuwang@zjut.edu.cn
* Correspondence: wangxq@zucc.edu.cn; Tel.: +86-137-5715-8022

Abstract: Scour leads to the loss of soil around monopile foundations for offshore wind turbines, which affects their structural safety. In this paper, the effect of scour on the lateral behaviour of monopiles was extensively investigated using finite element analysis, and calibration and comparison were undertaken using centrifuge tests. Piles with three slenderness ratios, i.e., 3, 5 and 8, were studied by keeping the diameter constant and varying the embedment length. Three scour types (local narrow, local wide and global) and four scour depths (0.5*D*, 1*D*, 1.5*D* and 2*D*; *D* signifies the pile diameter) were considered in this investigation. The results indicate that the lateral resistance of the pile is the greatest in the case of local narrow scour, followed by that in the cases of local wide scour and global scour. When the scour depth is larger than 1*D*, the influence of the scour type on the pile lateral bearing behaviour is insignificant. The influence of the scour type and scour depth on the pile lateral bearing behaviour is broadly similar for piles with slenderness ratios of 3, 5 and 8. However, the piles featured with smaller embedment lengths show a larger decrease rate in their lateral capacity, which means the effect of scour should cause more concern on small slenderness ratio monopiles.

Keywords: piles and piling; scour; finite element methods; centrifuge modelling; lateral bearing behaviour

check for updates

Citation: Li, Q.; Wang, X.; Gavin, K.; Jiang, S.; Diao, H.; Wang, M.; Wang, K. Scour Effect on the Lateral Bearing Behaviour of Monopiles Considering Different Slenderness Ratios. *Water* **2024**, *16*, 226. https://doi.org/10.3390/w16020226

Academic Editors: Xuguang Chen and Fayun Liang

Received: 13 December 2023
Revised: 29 December 2023
Accepted: 4 January 2024
Published: 9 January 2024

Copyright: © 2024 by the authors. Licensee MDPI, Basel, Switzerland. This article is an open access article distributed under the terms and conditions of the Creative Commons Attribution (CC BY) license (https://creativecommons.org/licenses/by/4.0/).

1. Introduction

As a result of the introduction of low-carbon green growth policies, many countries have mandated the increased production of renewable energy. In particular, 189 GW of wind installations produced 362 TWh electricity, covering 14% of EU's electricity demand, in 2018. Globally, offshore wind power is more welcomed than its onshore counterpart because of its abundant reserves, high energy density, reduced demand for land, as well as limited regulations [1]. Owing to their economical features, ease of design and simple manufacture and installation procedures, monopiles account for 81% of offshore wind foundations in Europe [2].

Monopiles in the offshore marine environment are prone to scour. The mechanism is that the soil within a certain area in the vicinity of the pile is washed away by waves and

current, reducing the lateral capacity of the pile and changing the structural stiffness and system frequency [3–15]. Two monopiles at the Robin Rigg wind farm were decommissioned after only six years of operation due to massive unexpected scour, demonstrating the hazard that the active marine environment poses to OWTs [16]. Research shows that the maximum scour depth is related to the pile diameter [17,18]. The scour depth normally falls in the range of 0.8–2.5D [19], where D is the pile diameter. With the advent of large-capacity offshore wind turbines, the diameter of the monopile foundation increases continuously, while the pile slenderness ratio (L/D) remains in a narrow range, typically from 3 to 6 [20]. As a result, the scour depth increases, intensifying its impact on the monopile foundation of the wind turbine [6]. More importantly, the monopile foundation is mainly designed to transmit the lateral load, and a significant amount of the load is resisted by the upper layer soil. Problems can be posed for the superstructure due to excessive fatigue stresses, as well as operational issues with the turbine. A tubular tower on a monopile foundation is more subjected to scour than a tripod foundation and a lattice tower with piles [19,21]. Therefore, it is of great importance to consider the effect of scour in the analysis and design of offshore wind turbine (OWT) monopile foundations without scour protection. The shapes of common types of scour holes are illustrated in Figure 1, where α denotes the scour slope angle, W_t denotes the top scour width, W_b denotes the bottom scour width, D_s denotes the scour depth and z denotes the depth below the original mudline.

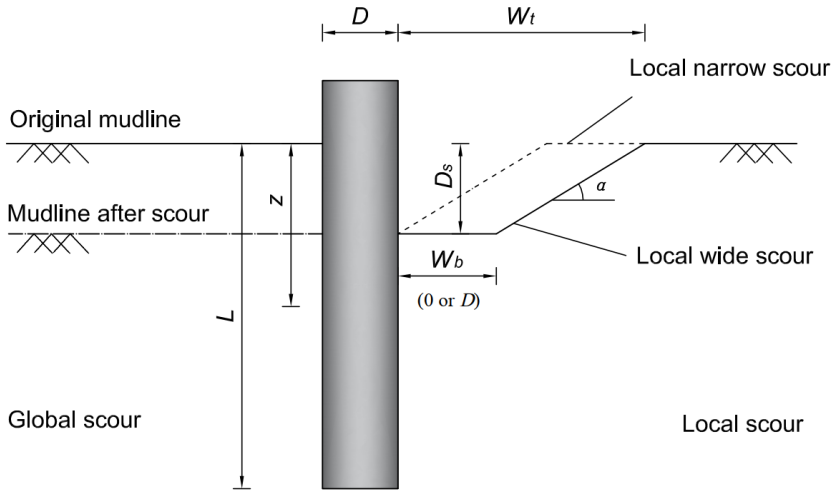

Figure 1. Symbols and definitions of scour holes (modified after Li et al. [22]).

Some previous works on the effect of scour on monopiles are detailed herein. Li et al. [23] extended a bridge scour model to predict deep water pile scour. The pile behaviour in the presence of scour was studied and the sensitive scour range for various types and sizes of offshore piles was identified. Considering the stress history effect on the behaviour of piles in sand under scour, Lin et al. [24] indicated that ignoring the stress history resulted in a conservative design. Achmus et al. [25] developed a three-dimensional finite element model to study the lateral deformation response of monopile foundations with scour under monotonic and one-way cyclic loading. With this model, a case study on a planned wind turbine in the Taiwan Strait was analysed, and the economic considerations of different design options were discussed. Mostafa [26] investigated the effect of local and global scour on the behaviour of laterally loaded piles installed under different soil conditions. Various parameters were analysed, such as soil type, scour depth, scour hole dimension, pile material, magnitude of lateral load and load eccentricity. The results show that scour has a significant impact on piles installed in sand and a less significant impact on piles installed in clay, and that global scour has a significant impact on the pile lateral displacement and bending stresses. The effect of scour is more significant if piles are subjected to large lateral loads due to the nonlinear response of the pile–soil system. The effect of scour in stiff clayey soils on piles is more pronounced than that in soft clayey soils.

Li et al. [27] calibrated a numerical model of a monopile in soft marine clay against field test data without scour and analysed several key factors relating to scour, such as the depth, width and slope of the scour hole, as well as the diameter and head fixity of the pile. The relationships of the ultimate lateral capacity of a monopile with the depth, width and slope angle of the scour hole were obtained. The numerical results show that scour depth has a more significant influence on the pile lateral capacity than scour width. In addition, a pile with a free head is more sensitive to scour than that with a fixed head. Sørensen and Ibsen [5] illustrated the effect of using design scour depths when designing for the ultimate limit state (ULS) and the fatigue limit state (FLS) by means of a desk study based on the statistical wave and current data at the Scroby Sands Offshore Wind Farm. The study does not provide guidelines for the design of monopile foundations exposed to scour. However, the desk study illustrates that scour hole backfilling can reduce stresses in the foundation, which indicates potential cost savings in the design process, if considered. The action of waves can densify redeposited soil. Prendergast et al. [4] attempted to monitor scour using a vibration-based method. A scale model test was used to measure the effect of scour on the natural frequency of a model monopile, and a spring–beam FE numerical model was developed to examine the foundation response. The results suggest that wind turbines founded in loose sand will exhibit the largest relative reduction in natural frequency resulting from scour, compared to those in denser deposits. Tang and Zhao [6] established a blade–tower–monopile integrated offshore wind turbine numerical model to explore the influence of scour on the dynamic characteristics of wind turbines considering parameters such as the blade azimuth, pitch angle, rotor speed and soil stiffness. The Modified Blade Element Momentum theory was used to calculate the wind load and obtain the impact of scour on the wind-induced response of a monopile wind turbine, considering the control system and aeroelastic coupling. Finally, a reference method was proposed for estimating the scour depth according to the monopile foundation offshore wind turbine wind-induced response. Li [1] carried out a series of centrifuge tests on a model monopile installed in dense sand with an embedment ratio of 5 to investigate the effect of the scour on the foundation lateral response. Three scour types (local narrow, local wide and global) and three scour depths (1D, 1.5D and 2D) were considered, which represent a range of common scour shapes in real engineering applications. The favourable effect of local scour types compared with the assumption of global scour conditions was evaluated using empirical equations, and the detrimental effect of an increased scour depth on the pile moment capacity was also assessed. To conclude, a significant amount of numerical and experimental research has been conducted to date, with limited studies considering the effect of the scour hole geometry on the lateral resistance of OWT monopiles with a relatively rigid behaviour (small L/D ratio).

This paper presents the results of centrifuge tests and finite element analysis for evaluating the effect of scour on the response of open-ended monopiles under lateral loading. Different parameters were considered, including load amplitude, scour depth, scour type and pile slenderness ratio (L/D). PLAXIS 3D [28] was used in the finite element analysis (FEA), and model calibration and comparison were conducted using centrifuge tests [1]. In all cases considered, the pile was embedded into homogeneous dry dense sand.

2. Centrifuge Tests

The testing programme comprises 10 tests: 1 monotonic load test with no scour (reference test) and 9 monotonic load tests with three scour types and three scour depths [1], which are briefly described in this section. The effects of global scour, local narrow scour and local wide scour were assessed at scour depths of 1D, 1.5D and 2D.

2.1. Model Pile and Soil Characterisation

The model pile was open-ended and fabricated from aluminium tube with an outer diameter (D) of 18 mm, a wall thickness (t) of 1 mm and a total length of 240 mm. A pile slenderness ratio (L/D) of 5 was achieved to keep in accordance with those typically used

in the real offshore environments. The primary dimensions and material properties of the pile can be found in Table 1. The scaling factor in length is set as 0.01 (i.e., the centrifuge acceleration rate is 100× *g*). The model pile was jacked into the sand sample prior to spinning up the sample (i.e., the pile was installed at 1× *g*).

Table 1. Model and corresponding prototype pile dimensions and properties (modified after Li [1]).

Property	Model Pile	Prototype Pile
Length (embedded + load eccentricity)	90 + 144 mm	9 + 14.4 m
Diameter, outer	18 mm	1.8 m
Wall thickness	1 mm	30 mm
Elasticity modulus (*E*)	70 GPa	210 GPa
Moment of inertia (*I*)	1936 mm^4	0.065 m^4
Bending stiffness (*EI*)	0.137 kPa·m^4	13.7 GPa·m^4
Material	aluminium	steel (assumed)

Note: Centrifuge tests were performed at 100× *g*.

The foundations were formed using dry Geba silica sand with an achieved relative density *RD* = 80%. The effective friction angle at a critical state ($\varphi\prime$) was determined to be 34°. The geotechnical characteristics of Geba sand are summarised in Table 2.

Table 2. Soil properties of Geba sand (Li et al. [22]; Maghsoudloo et al. [29]).

e_{min}	e_{max}	G_s	D_{50} (mm)	C_U	C_C
0.64	1.07	2.67	0.11	1.55	1.24

2.2. Centrifuge Loading Technique

A two-dimensional actuator was used to impose a lateral load (*H*) near the pile head, at a pre-determined height of *e* = 8*D* above the original ground surface, to mimic the lateral loading and significant overturning moment resulting from the combined action of wind, waves and current. The applied lateral load was measured using parallel beam load cells (HT Sensor Technology Co., Xi'an, China; TAL220; measuring range 100 N; sensitivity 0.05%), and the lateral displacement was measured near the pile head using the signal encoder of the actuator. The terminology used to describe the pile response is summarised in Figure 2; *L* refers to the embedded length of the pile, *e* is the loading eccentricity, R_0 is the distance from the pivot point to the toe of the pile, *H* is the applied lateral load, *y* is the lateral displacement of the pile at any height along the pile and θ is the rotation angle of the pile. The loading eccentricity, *e*, was maintained constant in all tests at 8*D*.

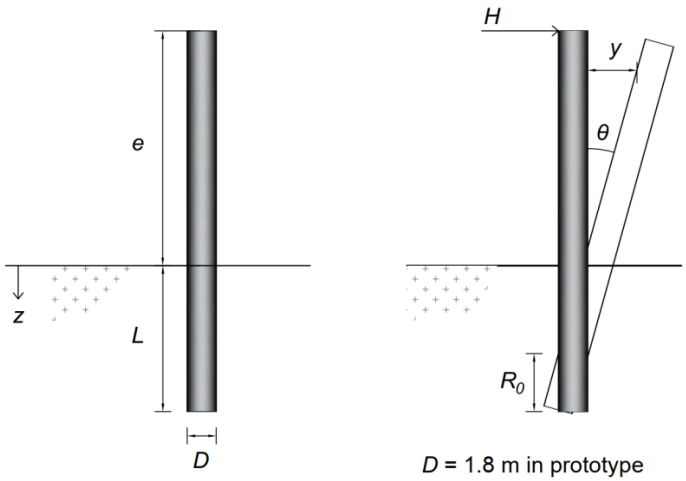

Figure 2. Sketch of pile (modified after Li [1]).

2.3. Scour Hole Formation and Testing Programme

For simplicity, a certain scour hole was determined according to three parameters, namely the scour type, scour depth and scour hole slope angle. The scour bottom width (W_b) was chosen at 0 and D used for differentiating between local narrow scour and local wide scour. The scour depth from 1D to 2D was especially evaluated, which covers the common scour depth range that a wind turbine most probably would encounter. The scour hole slope angle was kept constant at 30°, which is in line with previous experimental investigations [30,31].

Three scour depths, namely 1D, 1.5D and 2D, and three scour shapes, namely local narrow scour, local wide scour and global scour, were modelled (schematically shown in Figure 3). Global scour was modelled to fully remove the whole soil layer, resulting in a reduction in the effective stress at any (horizontal) distance away from the pile, representing soil erosion at a wide distance around the pile, which potentially occurs due to the natural seabed migration or scour around an entire wind farm. Local scour represents the case of a scour hole occurring in the direct vicinity of a pile, which results in a localised reduction in effective stress. Normally, the local scour hole is conical in shape with a trapezoidal cross-section. The bottom width of the scour hole was set as $W_b = 0$ for local narrow scour, and $W_b = D$ for local wide scour; therefore, the top width of the scour hole increased proportionally with the scour depth [1].

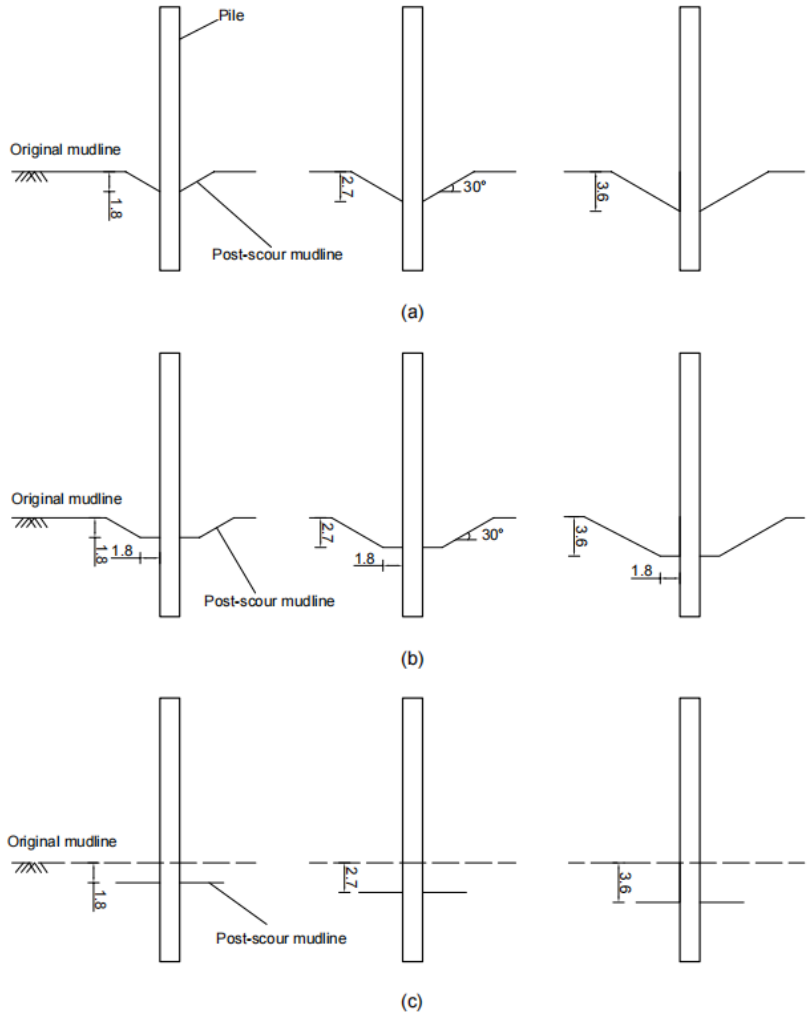

Figure 3. Schematic illustration of (**a**) local narrow scour; (**b**) local wide scour; (**c**) global scour (dimensions in prototype scale, m; modified from Li et al. [22]).

Following the creation of a scour hole (when relevant), the pile was pushed into the soil at 1 g using the vertical actuator operating at a model scale rate of 0.1 mm/s until the target embedment depth of $L = 5D$. Subsequently, the model was subjected to an enhanced centrifugal acceleration field of 100 g. A lateral load was applied to the pile head using lateral movement of the actuator at a constant model scale rate of 0.02 mm/s.

3. Finite Element Analysis

3.1. Mesh Details

The schematic three-dimensional FE mesh used for pile–soil interaction analysis is shown in Figure 4. To improve the computational efficiency, only half of the pile section in the direction of the load application was modelled. All numerical computations of the isoperimetric elements were performed using reduced numerical integration. The mesh dimensions and number of nodes and elements in the mesh were determined by performing a number of initial trial analyses with several meshes of increasing refinement (mesh density) until the resulting displacements and stresses around the pile no longer changed significantly with further refinement. The distances to the lateral rigid boundaries in the FEA are shown in Figure 4. A soil domain 20D in length, 10D in width and 2L in height was used for the simulation of the seabed. These dimensions were large enough to eliminate the boundary effect. The soil was simulated using 10-node tetrahedral elements and pile using 6-node plate elements. The mesh was highly refined around the pile and coarser near the boundary.

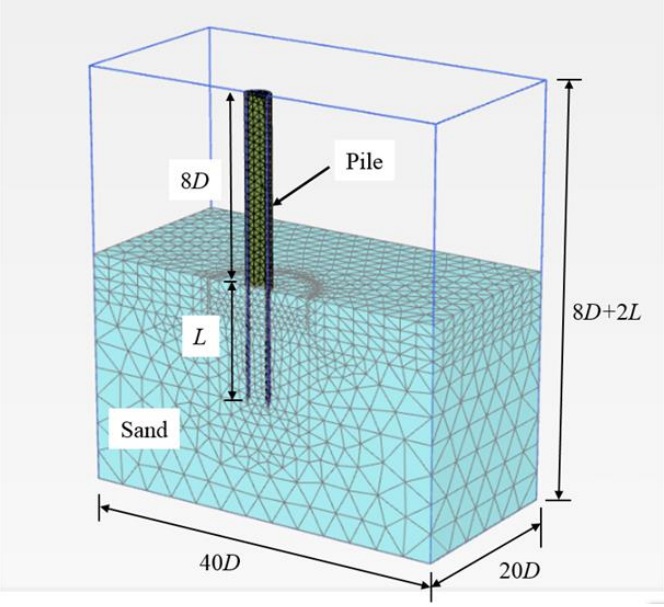

Figure 4. Typical mesh adopted in three-dimensional finite element analysis using PLAXIS.

All the nodes on the lateral boundaries were restrained from motion in the normal direction to the respective surfaces representing rigid, smooth lateral boundaries. All the nodes on the bottom surface were restrained in all three directions representing rough, rigid bottom surfaces.

3.2. Material Properties

The material behaviour of the pile was assumed to be linearly elastic with the parameters E = 210 GPa (Young's modulus) and ν = 0.3 (Poisson's ratio) for steel. The considered pile geometries are given in Table 3.

Table 3. Pile geometries.

No.	Materials -	Outer Diameter/*D* m	Length/*L* m	*L*/*D* Ratio -	Wall Thickness/*t* mm
1	Steel	1.8	5.4	3	30
2	Steel	1.8	9	5	30
3	Steel	1.8	14.4	8	30

One important issue in numerical modelling is to select the proper constitutive model and right related parameters. The Hardening Soil (HS) model [32] available in PLAXIS 3D CE V20 was featured with the stress dependency of the soil stiffness. For the special case of a drained triaxial test, the observed relationship between the axial strain and the deviatoric stress was approximated using a hyperbola. Konderner [33] was the first to formulate such a relationship and later Duncan and Chang [34] used it in the well-known hyperbolic model. Hardening Soil supersedes the hyperbolic model according to several characteristics: (i) using the theory of plasticity rather than the theory of elasticity; (ii) including soil dilatancy; (iii) introducing a yield cap.

The eight parameters related to the HS model were derived on the basis of the known relative density of sand from the empirical formulas reported by Brinkgreve et al. [35]. The model parameters were derived as follows:

The relative density (*RD*) is defined as $(e_{max} - e)/(e_{max} - e_{min})$, where e is the current void ratio of the sand specimen, e_{max} is the maximum void ratio (loosest packing) and e_{min} is the minimum void ratio (densest packing). The minimum and maximum void ratios of Geba sand were determined according to the Japanese Standard [36], as displayed in Table 2. The relative density, usually presented as a percentage, was used in this paper.

Before the parameters of the HS model were considered, the relative density was used to estimate the unit weight of sand:

$$\gamma = 15 + 4.0RD/100 \left[\mathrm{kN/m^3}\right] \quad (1)$$

The HS model involved three different stiffness parameters, each quantifying the reference stiffness in a particular stress path for a given reference stress level, p_{ref}. For sand, it was assumed that stiffness varied linearly with *RD*. The following formulas are proposed for the reference stiffness parameters, considering p_{ref} = 100 kN/m^2:

Secant stiffness for the CD triaxial test:

$$E_{50}^{ref} = 60000RD/100 \left[\mathrm{kN/m^2}\right] \quad (2)$$

Tangent oedometer stiffness:

$$E_{oed}^{ref} = 60000RD/100 \left[\mathrm{kN/m^2}\right] \quad (3)$$

Unloading reloading stiffness:

$$E_{ur}^{ref} = 180000RD/100 \left[\mathrm{kN/m^2}\right] \quad (4)$$

The actual stiffness is stress-dependent. The rate of stress dependency, m, is calculated using:

$$m = 0.7 - RD/320 \left[-\right] \quad (5)$$

ν_{ur}, Poisson's ratio for unloading and reloading, could be taken as 0.2.

The cohesion of sand was hypothesised to be 0 and the other strength-related properties were derived using:

$$\varphi\prime = 28 + 12.5RD/100 \left[^{o}\right] \quad (6)$$

$$\psi = -2 + 12.5RD/100 \left[^{o}\right] \quad (7)$$

Table 4 gives the deduced parameter values for the sand with a relative density (*RD*) of 80% by using the above formulas. An exact match could not be captured between the numerical and the physical modelling merely based on the deduced numerical parameters. Therefore, assisted by the centrifuge experiments, the author calibrated the soil model.

Table 4. Parameters for the HS model.

Parameter	Name	Brinkgreve et al. [35]	After Calibration	Unit
Unit weight	γ	18.2	15.57 (real value)	[kN/m^3]
(Effective) cohesion	c'_{ref}	0 (pre-defined)	0 (pre-defined)	[kN/m^2]
(Effective) angle of internal friction	$\varphi\prime$	38	34 (real value)	[°]
Angle of dilation	ψ	8	4 (real value)	[°]
Secant stiffness for CD triaxial test	E_{50}^{ref}	4.8×10^4	4.1×10^4	[kN/m^2]
Tangent oedometer stiffness	E_{oed}^{ref}	4.8×10^4	2.1×10^4	[kN/m^2]
Unloading reloading stiffness	E_{ur}^{ref}	1.44×10^5	1.23×10^5	[kN/m^2]
Power of stress-level dependency of stiffness	m	0.45	0.5	[-]
Poisson's ratio for unloading–reloading	ν'_{ur}	0.2	0.2	[-]
Reference stress for stiffnesses	p^{ref}	100	100	[kN/m^2]
Failure ratio	R_f	0.9	0.9	[-]
K_0-value for normal consolidation	K_0^{nc}	0.4408	0.4408	[-]

3.3. Modelling of Scour and Parametric Case Studies

To cover the main range of expected scour hole geometries and ensure consistency with the centrifuge tests, three scour hole shapes (one for global scour and two for local scour) were established, as shown in Figure 3. The common extreme scour depth is within two times the pile diameter [17,18,37]; thus, scour hole depths equivalent to 0.5, 1, 1.5 and 2 times the pile diameter were considered (i.e., Ds/D = 0.5, 1, 1.5, 2) in this FEA scheme. The pile L/D ratio was varied by keeping the pile diameter constant while changing the pile length. For consistency with the centrifuge tests, dry sand was simulated in all of the numerical modelling.

The analysis was performed using the load control method to evaluate the lateral displacement developed under various load magnitudes. The pile lateral load–displacement with different scour types (local narrow scour, local wide scour and global scour) and depths (0, 0.5D, 1D, 1.5D and 2D) was analysed. The influence of the pile slenderness ratio (L/D = 3, 5 and 8) on the pile lateral bearing behaviour was evaluated. The lateral bearing capacity (H_{ult}) of the pile was determined as the lateral load which caused a lateral displacement equating to 0.1D at the original mudline, identical with the centrifuge experiments.

The FE calculations were executed in several phases. Firstly, the initial stress state in the system caused by the self-weight of the soil was generated using soil elements only. Subsequently, the pile was activated and 'wished in place', i.e., the installation process of the pile was not modelled. Scour was created by de-activating the soil elements inside the designed scour hole. The lateral load was applied and increased according to the proper load intervals.

4. Analysis and Results

4.1. Model Calibration

The numerical model calibration was performed based on the work of Brinkgreve et al. [28] and centrifuge monotonic loading tests in the case of the absence of scour, as shown in Figure 5. The load and displacement values were obtained at the mudline level. The combination of the soil parameters that fitted best the centrifuge experiments was identified, as presented in Table 4.

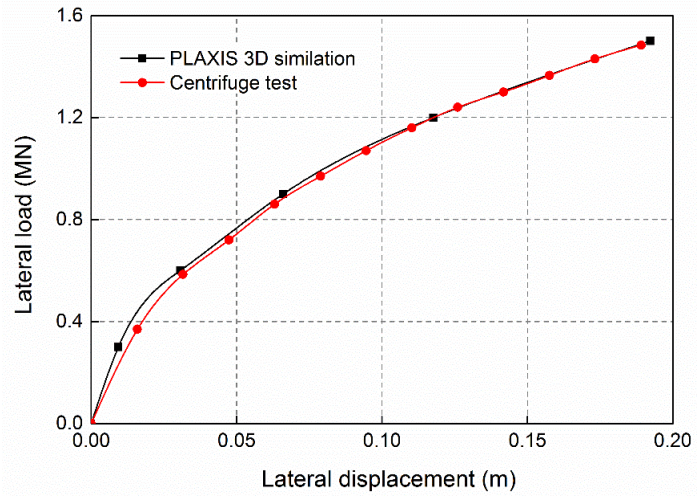

Figure 5. Calibration with the load–displacement curves for the no scour centrifuge experiment and the equivalent numerical analysis.

4.2. Effect of Scour Depth

The simulation results of the lateral load versus lateral displacement relationship under different scour depths are presented in Figure 6: (a) local narrow scour, (b) local wide scour and (c) global scour. The pile had an L/D ratio of 5. As can be seen from the figure, a nonlinear load–displacement response was observed, and the nonlinearity became even more obvious at the larger scour depths. With an increase in scour depth, the stiffness of the load–displacement response and the pile resistance decreased. The influence of scour depth on the lateral capacity could be estimated from the lateral load–displacement curves presented in the figure.

The effect of scour on the pile lateral load–displacement relationships observed for the piles with L/D ratios of 3 and 8 was very similar to that for the pile with an L/D ratio of 5 (Figure 6). For this reason, only the lateral load–displacement curves of the pile with an L/D ratio of 8 are presented hereafter (in Figure 7). The lateral resistance of the pile with an L/D ratio of 8 was significantly higher than that of the pile with L/D ratio of 5, at any scour depth and for any scour type.

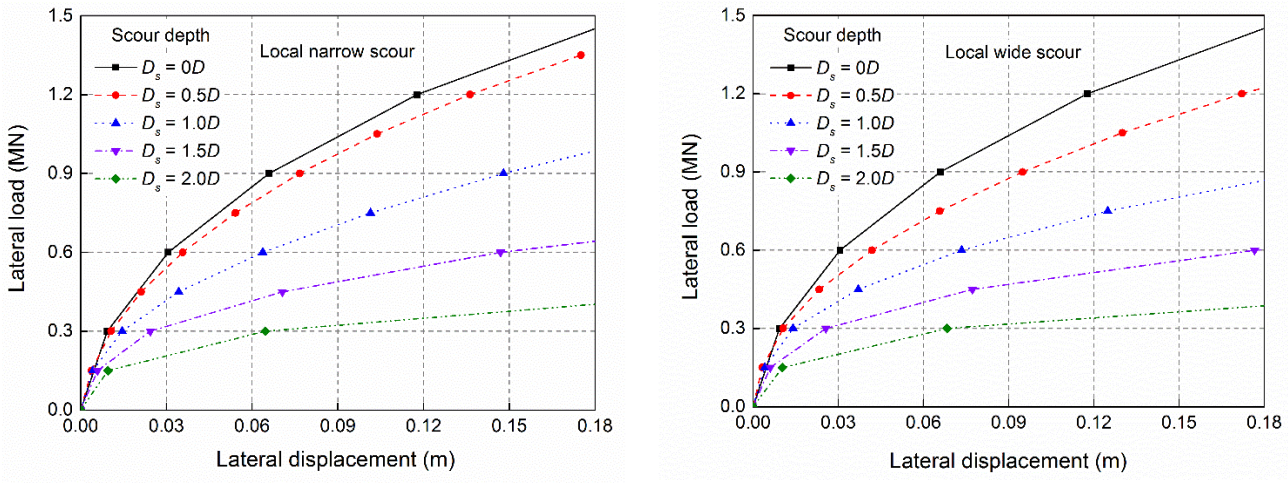

(**a**) (**b**)

Figure 6. *Cont.*

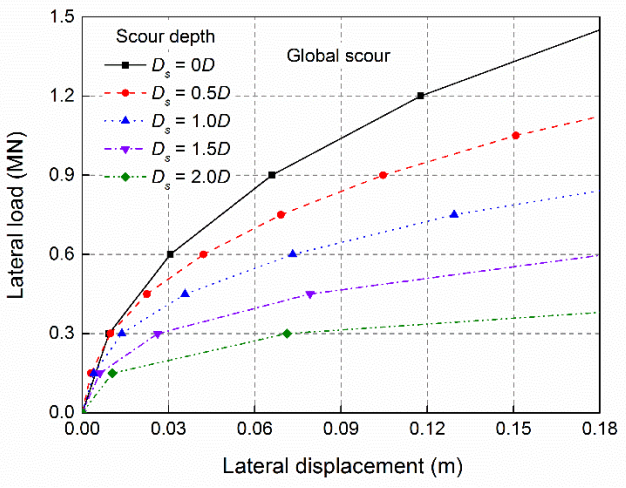

(**c**)

Figure 6. Pile lateral load–displacement relationships at different scour depths for cases of: (**a**) local narrow scour; (**b**) local wide scour; (**c**) global scour (L/D = 5).

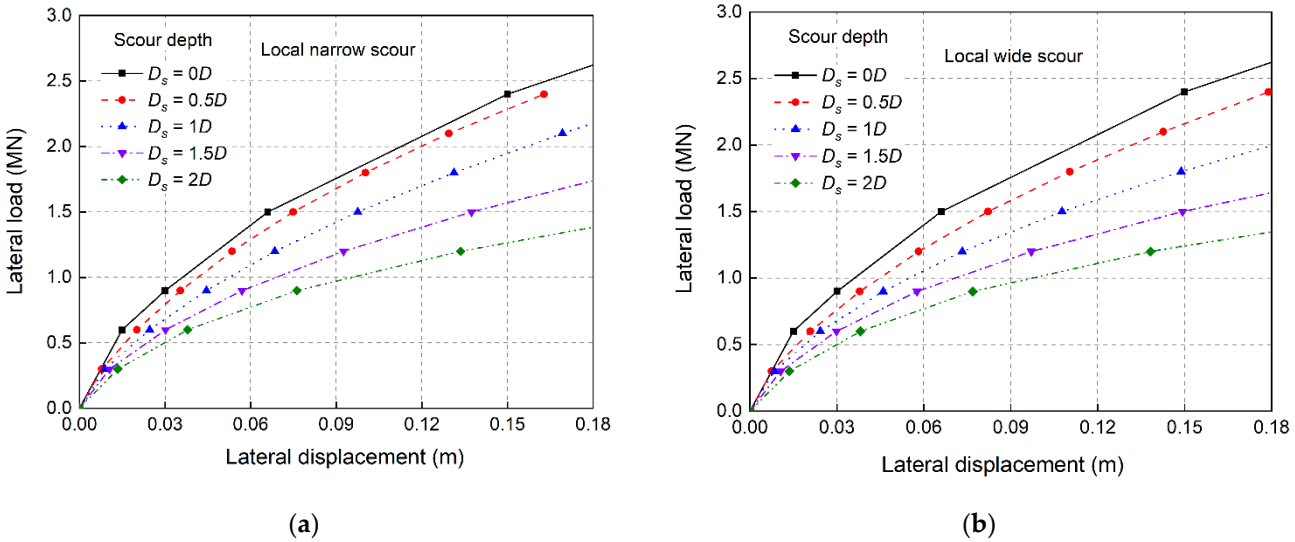

(**a**) (**b**)

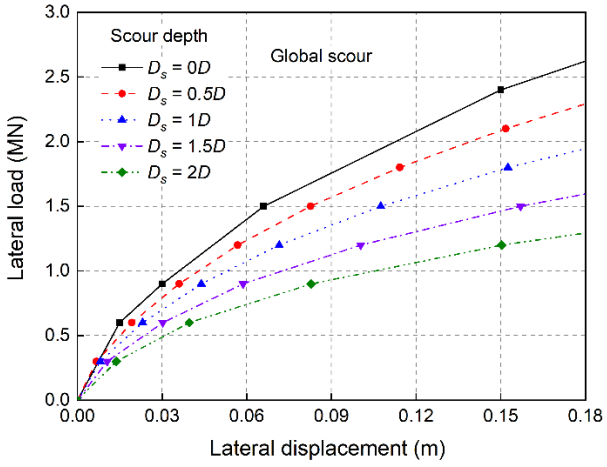

(**c**)

Figure 7. Pile lateral load–displacement relationships at different scour depths for cases of: (**a**) local narrow scour, (**b**) local wide scour; (**c**) global scour (L/D = 8).

Figure 8 shows the variation in the lateral bearing capacity (H_{ult}) of a monopile with the scour depth considering piles with L/D ratios of 3, 5 and 8. The lateral bearing capacity of the piles decreased almost linearly with the increase in scour depth for all the three scour types and all the three L/D ratios investigated.

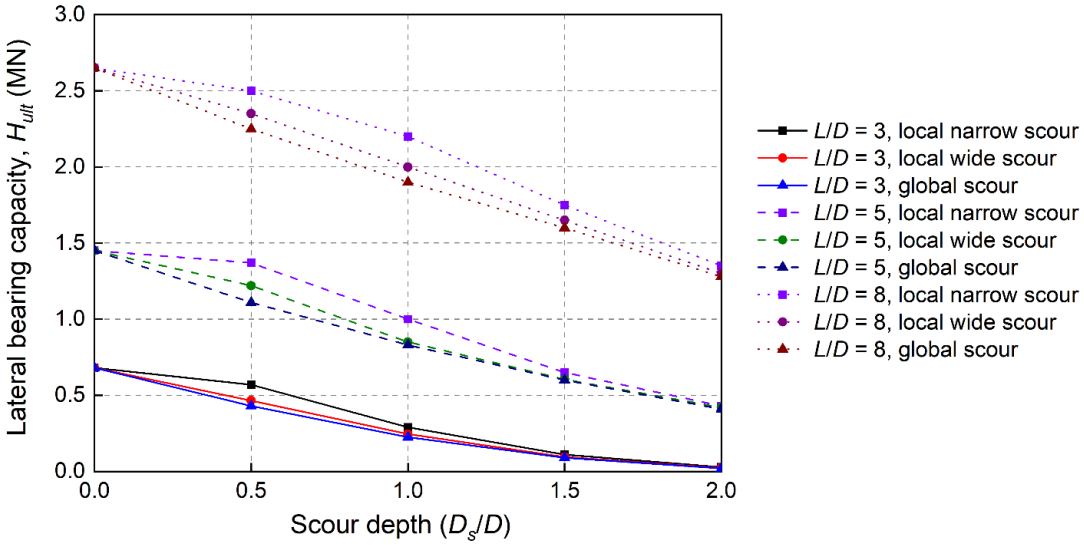

Figure 8. Relationships of pile lateral bearing capacity and normalised scour depth.

In order to compare the effect of scour on the pile lateral bearing capacity with regard to different slenderness ratios, the pile lateral bearing capacity can be expressed in terms of a dimensionless parameter:

$$R_s = \frac{H_s}{H_n} \tag{8}$$

where R_s is the lateral pile capacity ratio considering the effect of scour, H_s is the lateral bearing capacity under the influence of scour and H_n is the lateral bearing capacity without the influence of scour.

Figure 9 shows the lateral pile capacity ratio versus the normalised scour depth, with respect to different pile slenderness ratios. Firstly, scour could significantly decrease the lateral pile capacity. For example, for the pile with an L/D ratio of 5 under global scour, with the increase in scour depth from 0.5 to 2D, the lateral pile capacity ratios were 76.6%, 57.2%, 41.4% and 28.3%, which means that the lateral resistance of the pile decreased by 42.8% at the scour depth 1D and the reduction increased to 71.7% at the scour depth 2D. The reduced capacity was mainly attributed to the loss of the soil support around the pile, as the upper layer soil provides a significant amount of lateral resistance according to the classical p–y (soil reaction–pile lateral displacement) theory in monopile design [1].

Moreover, the influence of the scour depth on the lateral pile capacity ratio was more pronounced on the rigid pile. As can be clearly seen from Figure 9, the pile featuring a smaller embedment depth (signified by a smaller L/D ratio) witnessed a sharp decline in the lateral bearing capacity ratio at the same scour depth. Under the condition of local narrow scour, the lateral bearing capacity ratios of the piles with L/D ratios of 3, 5 and 8 at a scour depth of 1D were approximately 42.6%, 69% and 83% of that without scour, respectively. The lateral bearing capacity of the pile with L/D ratios of 3, 5 and 8 decreased by about 57.3%, 31% and 17%, respectively. Similarly, under the condition of local narrow scour, the reduction in the lateral bearing capacity sharply increased to approximately 95.9%, 70.3% and 49.1% corresponding to pile L/D ratios of 3, 5 and 8, respectively, at the scour depth 2D. The piles experienced similar trends under the condition of local wide scour and global scour. To conclude, the lateral capacity reduction caused by scour was fatal to the lateral resistance of the offshore wind turbines with monopile foundations.

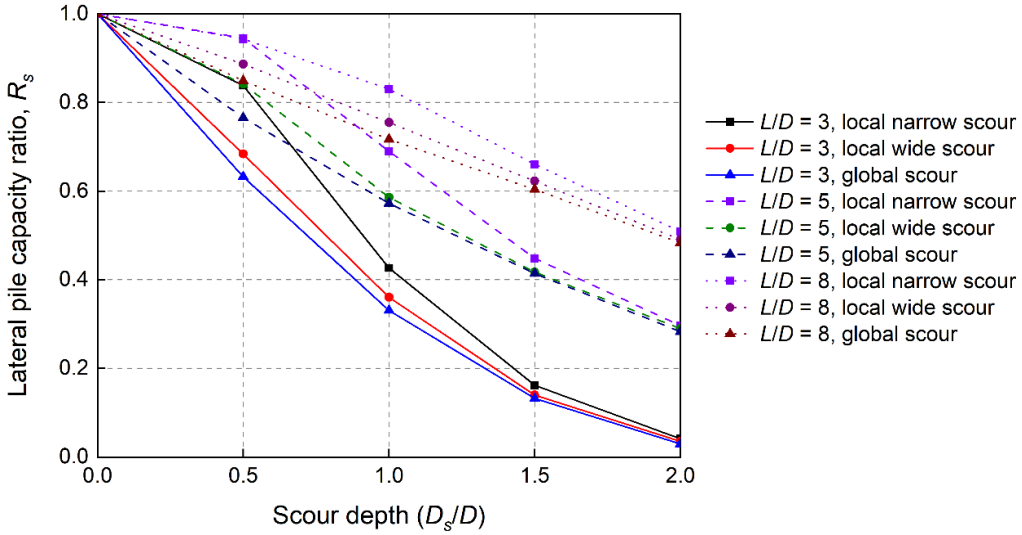

Figure 9. Lateral pile capacity ratio versus normalised scour depth.

The difference in the lateral pile capacity ratio caused by the pile L/D ratios under scour was attributable to the fact that the larger L/D ratio a pile has, the larger its embedment length is. The sand loss ratio due to scour of a long pile is smaller than that of a short pile, thus showing a smaller decrease in the lateral bearing capacity. Detailed information on the lateral pile capacity ratio for all the three scour types and three pile L/D ratios is listed in Table 5.

Table 5. Lateral pile capacity ratio (R_s) considering the effect of scour.

D_s	L/D = 3			L/D = 5			L/D = 8		
	Local Narrow	**Local Wide**	**Global**	**Local Narrow**	**Local Wide**	**Global**	**Local Narrow**	**Local Wide**	**Global**
0	1	1	1	1	1	1	1	1	1
0.5D	0.838	0.684	0.632	0.945	0.841	0.766	0.943	0.887	0.849
1D	0.426	0.360	0.331	0.690	0.586	0.572	0.830	0.755	0.717
1.5D	0.162	0.140	0.132	0.448	0.417	0.414	0.660	0.623	0.604
2D	0.041	0.035	0.029	0.297	0.290	0.283	0.509	0.491	0.483

4.3. Effect of Scour Type

As mentioned earlier, three scour types, namely local narrow scour, local wide scour and global scour, were considered in this study. The general scour hole shapes are illustrated and related symbols are defined in Figure 1.

Figure 10 shows the lateral load–displacement relationships influenced by the scour types, at the scour depths (a) 0.5D, (b) 1D, (c) 1.5D and (d) 2D. The pile had a slenderness ratio of 5. It can be seen from the figure that scour type had a more significant effect on the lateral response of the pile at a shallower scour depth ($D_s \leq 1D$). The pile experiencing local narrow scour exhibited a stiffer load–displacement response than local wide scour. The major consequential difference was speculated as the amount of overburden pressure near to the pile. A pile experiencing local wide scour always showed a stiffer load–displacement response than global scour, due to the higher overburden pressure provided by the soil above the global scour mudline and the resistance provided by the sand slope near to the pile. Under the condition of local wide scour, compared with local narrow scour, the scour slope was farther away from the pile, with a smaller load–displacement response. In the case of global scour, there was no overburden effect compared with that in the case of the local scour types, in which case the pile showed the least stiffness in the load–displacement response, implying that assuming the removal of the whole soil layer above the scour depth

(global scour) is a conservative method considering the scour type effect up to a scour depth of 1*D*.

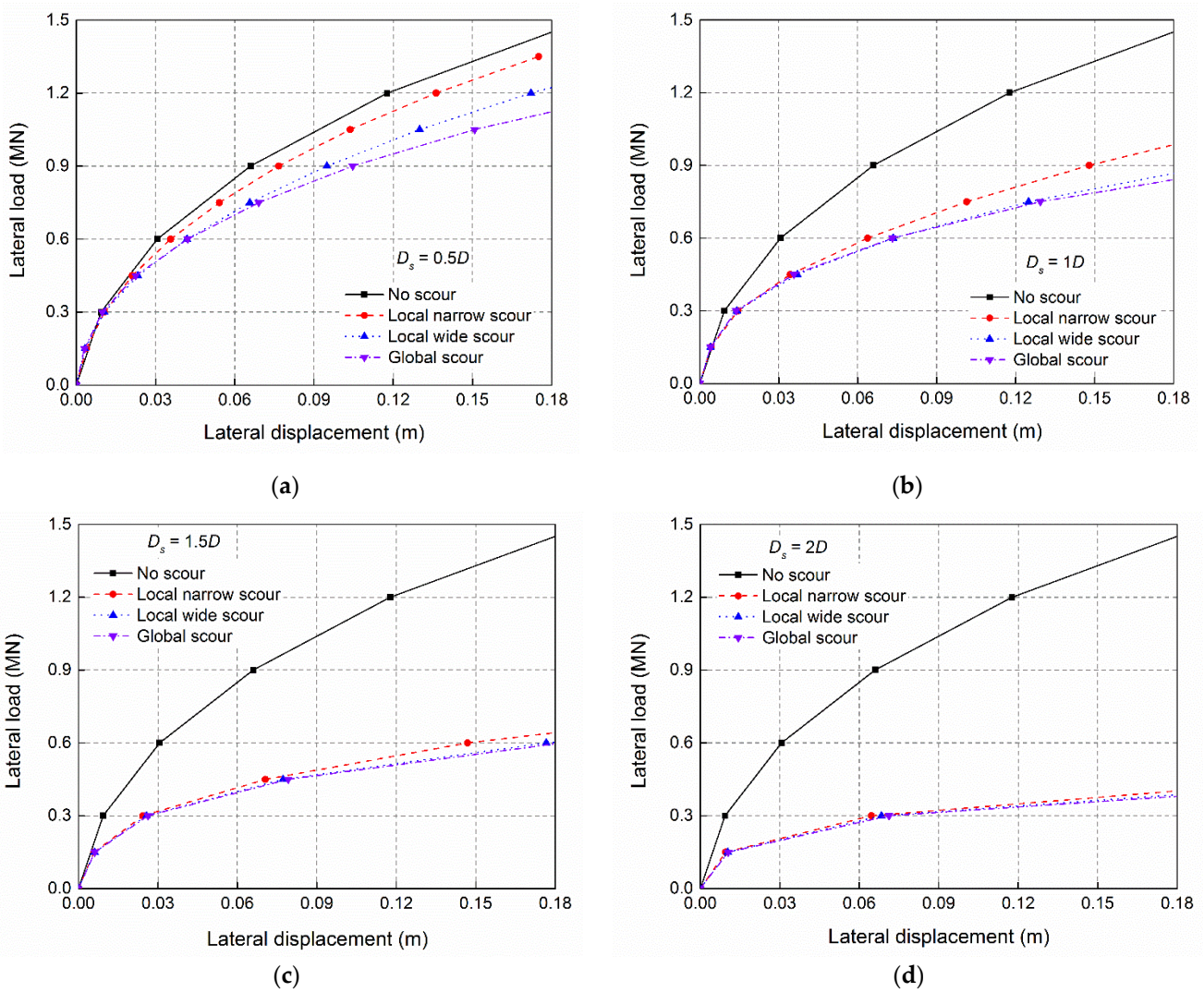

Figure 10. Effect of scour type on lateral load–displacement relationships at various scour depths: (**a**–**d**) scour depths equal to 0.5*D*, 1*D*, 1.5*D*, 2*D* (L/D = 5).

As the scour depth increased (D_s > 1*D*), the pile lateral load–displacement curves under the condition of local narrow scour became stiffer than those under the conditions of local wide scour and global scour, making it more difficult to distinguish the pile lateral load–displacement curves under local wide scour and global scour. The insignificant effect between local wide scour and global scour at a large scour depth (D_s > 1*D*) might result from the diminishing of the overburden effect of local wide scour compared with global scour.

The influence of the scour type effect on the lateral load–displacement relationship of a pile could also be observed for the piles with L/D ratios of 3 and 8. Therefore, only the lateral load–displacement curves for a pile with an L/D ratio of 8 are presented hereafter (in Figure 11).

The influence of the scour type on the lateral bearing capacity can be deduced from Figure 8. For the piles with L/D ratios of 3, 5 and 8, the capacity of the pile was the largest under local narrow scour, closely followed by those under local wide scour and global scour. The influence of the scour type on the lateral pile capacity was more significant at a scour depth less than 1*D*. With a further increase in the scour depth (D_s > 1*D*), the influence of the

scour type on the pile lateral bearing capacity was gradually minimised. The lateral bearing capacity in the case of local narrow scour was higher than that in the case of local wide scour and global scour, while the pile lateral capacities under local wide scour and global scour are very close to each other. From Table 5, the pile with an L/D ratio of 5 showed lateral capacity ratios of 69%, 58.6% and 57.2% at a scour depth of 1D corresponding to local narrow scour, local wide scour and global scour, respectively. Meanwhile, at a scour depth of 2D, the corresponding values were 29.7%, 29.0% and 28.3%. It can be concluded that at scour depths of 1.5D and 2D, the scour type no longer had significant effects on the lateral pile capacity ratio. Comparing Figures 10 and 11, the pile featured with a small slenderness ratio was more likely to be affected by the scour type.

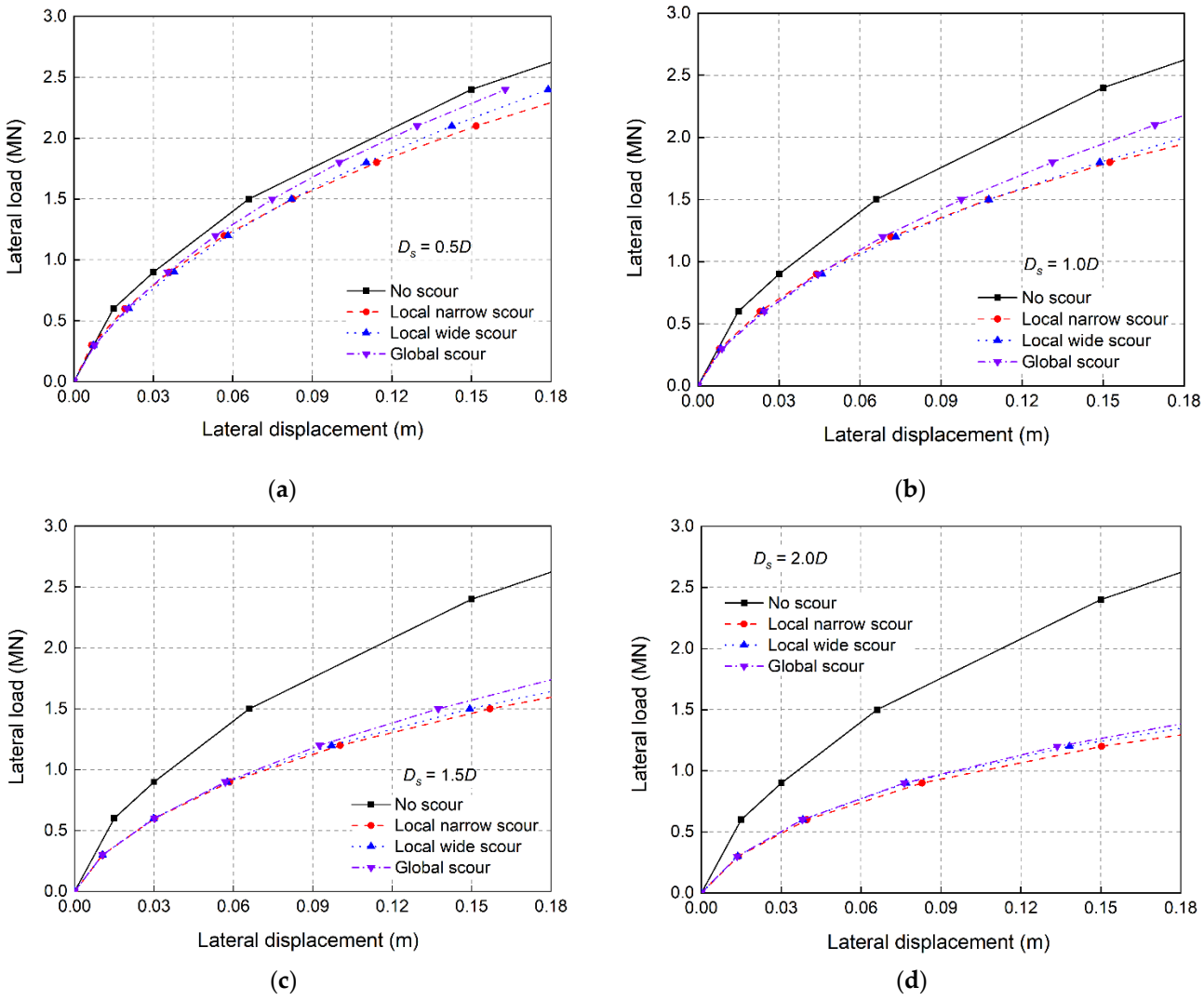

Figure 11. Effect of scour type on lateral load–displacement relationships at various scour depths: (**a**–**d**, scour depths equal to 0.5D, 1D, 1.5D, 2D) (L/D = 8).

4.4. Comparison between Centrifuge Tests and Finite Element Analysis

Li [1] reported centrifuge tests on a pile with a slenderness ratio (L/D) of 5, and the sand material and loading conditions are the same compared with this finite element modelling work. Figure 12 compares the lateral pile capacity ratio versus the normalised scour depth between the finite element modelling results of this study and the experimental results obtained by Li [1] on a pile with a slenderness ratio of 5.

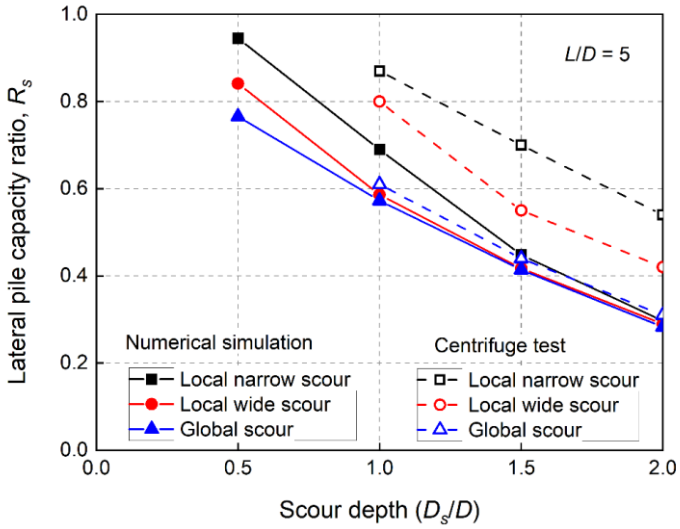

Figure 12. Lateral pile capacity ratio versus normalised scour depth (pile L/D = 5).

As can be seen from the comparison presented in Figure 12, the lateral pile capacity ratio versus the scour depth investigated in this study was generally comparable to that obtained by Li [1]. The pile capacity ratio decreased significantly with an increase in scour depth in both cases (FEA and centrifuge tests). The curves for global scour between the FEA and centrifuge tests were close to each other. However, the centrifuge test results showed a much higher lateral pile capacity ratio than those of the FEA in the case of both local wide scour and local narrow scour. It is impossible to compare these one by one because of the difficulties in controlling parameters (e.g., modelling scour holes, selecting soil parameters) between experimental techniques and numerical techniques. From the FEA, when the scour depth was larger than 1D, global scour could be taken as a general design case. However, from the centrifuge test perspective, it would be too conservative to take scour as the removal of the entire soil layer (global scour), even at a scour depth of 2D. For example, at D_s = 2D, the pile under local narrow scour had a lateral pile capacity ratio of 0.55, compared with that under local wide scour (0.42) and global scour (0.32), meaning at D_s = 2D, the pile capacities under local narrow scour and local wide scour were 72% and 31% larger than that under global scour. Therefore, FEA alone might be insufficient to quantify the effect of local scour shapes on the lateral pile response. More numerical and experimental work is encouraged to be carried out and model parameters need to be properly selected to improve the precision of FEA.

5. Conclusions

The effect of scour of the seabed on the lateral response of monopiles is an important subject for the safe operation of offshore wind turbines. Three-dimensional FEA was conducted in this study on piles with various slenderness ratios to investigate the effect on the lateral response of monopiles. For the convenience of practical application, three idealised scour types (local narrow scour, local wide scour and global scour) and four scour depths (0.5D, 1D, 1.5D and 2D) were considered, which covers the common scour shapes in engineering projects. Finite element modelling was calibrated, and the modelling results were compared with centrifuge test results. The following conclusions can be drawn from this study:

Scour has a significant deleterious effect on the lateral bearing behaviour of monopiles. With an increase in scour depth, the lateral bearing resistance decreases, while the lateral displacement of monopiles increases. Under the condition of local narrow scour, the lateral bearing capacity ratios of the piles with L/D ratios of 3, 5 and 8 at a scour depth of 1D decreased by about 57.3%, 31% and 17%, respectively. Correspondingly, the reduction in the lateral bearing capacity ratios sharply increased to approximately 95.9%, 70.3% and

49.1% at the scour depth 2D. The lateral pile capacity ratio decreases almost linearly with an increase in scour depth, which is broadly similar to that of the piles with slenderness ratios of 3, 5 and 8, regardless of the scour types. However, when the pile diameter is fixed, the lateral bearing capacity of the piles featured with small slenderness ratios declines more significantly, which means that the effect of scour should be considered more for a monopile foundation with a smaller slenderness ratio.

The scour type shows an inconsistent effect on the lateral load–displacement response and lateral pile capacity (ratio) at different scour depths. The effect of the scour type on the lateral response of a pile is more significant at a shallow scour depth ($D_s \leq 1D$). The lateral resistance of the pile is the greatest in the case of local narrow scour, followed by that in the case of local wide scour and global scour. When the scour depth (D_s) is larger than 1D, the influence of the scour type on the lateral pile capacity (ratio) is insignificant. For example, the pile with an L/D ratio of 5 showed lateral capacity ratios of 69%, 58.6% and 57.2% at a scour depth of 1D corresponding to local narrow scour, local wide scour and global scour, respectively. Meanwhile, at a scour depth of 2D, the corresponding values were 29.7%, 29.0% and 28.3%. To facilitate its design, when a large scour depth is to be considered (for example, $D_s > 1D$), it is rational to take global scour as the general design case. A very similar phenomenon can be observed for piles with slenderness ratios of 3, 5 and 8 in terms of the influence of the scour type on the lateral bearing behaviour, at any scour depth (0.5D, 1D, 1.5D and 2D). A pile featured with a small slenderness ratio is more influenced by scour type at the same scour depth.

Comparing the relationships of the lateral pile capacity ratio to the normalized scour depth between the FEA results of this study and the experimental results from Li [1] on a pile with a slenderness ratio of 5, the relationships between the FEA and centrifuge tests under global scour fit with each other quite well, while the centrifuge tests show a much higher lateral pile capacity ratio than the FEA in the case of local wide scour and local narrow scour. More research, both numerical and experimental, needs to be carried out to more accurately evaluate the effect of local scour shapes on the lateral bearing response of piles.

Author Contributions: Conceptualization, Q.L., X.W. and K.G.; methodology, Q.L. and M.W.; software, S.J. and H.D.; investigation, Q.L. and K.W.; validation, S.J. and M.W.; writing—original draft preparation, Q.L. and H.D.; writing—review and editing, X.W. and K.G.; supervision, X.W. and K.G.; funding acquisition, X.W., H.D. and K.W. All authors have read and agreed to the published version of the manuscript.

Funding: National Natural Science Foundation of China (NSFC) (Grant Nos. 52278373 and 52009122), Zhejiang Provincial Natural Science Foundation of China (Grant No. LQ21E090002), Zhejiang Engineering Research Centre of Intelligent Urban Infrastructure (IUI2022-ZD-01 and IUI2023-ZD-02), China Scholarship Council (CSC) and Section of Geo-Engineering, the Delft University of Technology.

Data Availability Statement: Data will be made available on request.

Acknowledgments: The authors would like to acknowledge the support of the Section of Civil Engineering, Hangzhou City University, and the Section of Geo-Engineering, the Delft University of Technology, and the funding from the CSC.

Conflicts of Interest: The author Qiang Li was employed by PowerChina Huadong Engineering (Shenzhen) Corporation Limited and Shengxiang Jiang and Mingyuan Wang were employed by the company PowerChina Huadong Engineering Corporation Limited. The remaining authors declare that the research was conducted in the absence of any commercial or financial relationships that could be construed as a potential conflict of interest.

Nomenclature

C_C	curvature coefficient
C_U	uniformity coefficient
c'_{ref}	(effective) cohesion

D	pile outer diameter
D_{50}	average grain size
D_s	scour depth
E	elasticity modulus
E_{50}^{ref}	secant stiffness for CD triaxial test
E_{oed}^{ref}	tangent oedometer stiffness
E_{ur}^{ref}	unloading–reloading stiffness
e	loading eccentricity
e_{max}	maximum void ratio of sand
e_{min}	minimum void ratio of sand
EI	bending stiffness
G_s	specific gravity
g	gravitational acceleration rate
H	lateral load
H_n	lateral bearing capacity without the influence of scour
H_s	lateral bearing capacity under the influence of scour
H_{ult}	lateral bearing capacity
I	moment of inertia
K_0^{nc}	K_0-value for normal consolidation
L	pile embedded length
m	power of stress-level dependency of stiffness
p	soil reaction
p^{ref}	reference stress for stiffness
R_0	distance from the pivot point to the toe of the pile
R_f	failure ratio
R_s	lateral pile capacity ratio considering the effect of scour
RD	relative density
t	pile wall thickness
W_b	bottom scour width
W_t	top scour width
y	lateral displacement of the pile
z	depth below original mudline
α	scour slope angle
θ	rotation angle of the pile
$\varphi\prime$	(effective) angle of internal friction
ψ	angle of dilation
γ	unit weight of sand
ν	Poisson's ratio
ν'_{ur}	Poisson's ratio for unloading–reloading
EU	European Union
FEA	finite element analysis
FLS	fatigue limit state
HS	Hardening Soil
OWT	offshore wind turbine
ULS	ultimate limit state

References

1. Li, Q. Response of Monopiles Subjected to Combined Vertical and Lateral Loads, Lateral Cyclic Load, and Scour Erosion in Sand. Ph.D. Thesis, Delft University of Technology, Delft, The Netherlands, 2020. [CrossRef]
2. Komusanac, I.; Brindley, G.; Fraile, D.; Ramirez, L. Wind Energy in Europe. 2021 Statistics and the Outlook for 2022–2026. Technical Report. 2022. Available online: https://www.anev.org/wp-content/uploads/2022/02/220222-Stats-Outlook.pdf (accessed on 3 December 2023).
3. Prendergast, L.J.; Reale, C.; Gavin, K. Probabilistic examination of the change in eigenfrequencies of an offshore wind turbine under progressive scour incorporating soil spatial variability. *Mar. Struct.* **2018**, *57*, 87–104. [CrossRef]
4. Prendergast, L.J.; Gavin, K.; Doherty, P. An investigation into the effect of scour on the natural frequency of an offshore wind turbine. *Ocean Eng.* **2015**, *101*, 1–11. [CrossRef]
5. Sørensen, S.P.H.; Ibsen, L.B. Assessment of foundation design for offshore monopiles unprotected against scour. *Ocean Eng.* **2013**, *63*, 17–25. [CrossRef]

6. Tang, D.; Zhao, M. Scour Effect on Dynamic Characteristics and Responses of Offshore Wind Turbines. *Comput. Model. Eng. Sci.* **2020**, *124*, 433–457. [CrossRef]
7. Zhang, F.; Dai, G.; Gong, W. Analysis solution of the lateral load response of offshore monopile foundations under asymmetric scour. *Ocean Eng.* **2021**, *239*, 109826. [CrossRef]
8. Harris, J.; Whitehouse, R.; Tavouktsoglou, N.; Godinho, P. Foundation scour as a geohazard. *J. Waterw. Port Coast. Ocean Eng.* **2019**, *6*, 145. [CrossRef]
9. Hucker, N.; Ward, I.; Manceau, S. Measured changes in the natural frequency of offshore wind turbines with monopile foundations. In Proceedings of the SECED: Conference in Earthquake Risk and Engineering towards a Resilient World 2019, London, UK, 9–10 September 2019.
10. Mayall, R.O.; McAdam, R.A.; Whitehouse, R.J.S.; Burd, H.J.; Byrne, B.W.; Heald, S.G.; Sheil, B.B.; Slater, P.L. Flume tank testing of offshore wind turbine dynamics with foundation scour and scour protection. *J. Waterw. Port Coast. Ocean Eng.* **2020**, *146*, 04020033. [CrossRef]
11. Dai, S.; Han, B.; Wang, B.; Luo, J.; He, B. Influence of soil scour on lateral behavior of large-diameter offshore wind-turbine monopile and corresponding scour monitoring method. *Ocean Eng.* **2021**, *239*, 109809. [CrossRef]
12. Jiang, W.; Lin, C.; Sun, M. Seismic responses of monopile-supported offshore wind turbines in soft clays under scoured conditions. *Soil Dyn. Earthq. Eng.* **2021**, *142*, 106549. [CrossRef]
13. Jiang, W.; Lin, C. Lateral responses of monopile-supported offshore wind turbines in sands under combined effects of scour and earthquakes. *Soil Dyn. Earthq. Eng.* **2022**, *155*, 107193. [CrossRef]
14. Lin, Y.; Lin, C. Scour effects on lateral behavior of pile groups in sands. *Ocean Eng.* **2020**, *208*, 107420. [CrossRef]
15. Chen, S.; Gong, E.; Zhao, X.; Arikawa, T.; Chen, X. Large-scale experimental study on scour around offshore wind monopiles under irregular waves. *Water Sci. Eng.* **2022**, *15*, 40–46. [CrossRef]
16. Carlos, M.V.; Susana, L.Q.; Bhattacharya, S.; Simons, R. Numerical study on the effects of scour on monopile foundations for Offshore Wind Turbines: The case of Robin Rigg wind farm. *Soil Dyn. Earthq. Eng.* **2023**, *167*, 107803. [CrossRef]
17. Sumer, B.M.; Fredsøe, J.; Christiansen, N. Scour around vertical pile in waves. *J. Waterw. Port Coast. Ocean Eng.* **1992**, *118*, 15–31. [CrossRef]
18. *Offshore Standard DNV-OS-J101 6*; Design of Offshore Wind Turbine Structures. Det Norske Veritas: Bærum, Norway, 2004.
19. Zaaijer, M.B.; Tempel, J. Scour protection, a necessity or a waste of money. In Proceedings of the 43 IEA Topixal Expert Meeting, Skaerbaek, Denmark, 9–10 March 2004; pp. 43–51.
20. Arany, L.; Bhattacharya, S.; Macdonald, J.; Hogan, S. Design of monopiles for offshore wind turbines in 10 steps. *Soil Dyn. Earthq. Eng.* **2017**, *92*, 126–152. [CrossRef]
21. Tempel, J.; Zaaijer, M.B.; Subroto, H. The effects of scour on the design of offshore wind turbines. In Proceedings of the 3rd International Conference on Marine Renewable Energy, London, UK, 7–9 July 2004; pp. 27–35.
22. Li, Q.; Askarinejad, A.; Gavin, K. The impact of scour on the lateral resistance of wind turbine monopiles: An experimental study. *Can. Geotech. J.* **2020**, *58*, 1770–1782. [CrossRef]
23. Li, Y.; Chen, X.; Fan, S.; Briaud, J.L.; Chen, H.C. Is scour important for pile foundation design in deepwater? In Proceedings of the 2009 Offshore Technology Conference, Houston, TX, USA, 4–7 May 2009; pp. 1–12.
24. Lin, C.; Bennett, C.; Han, J.; Parsons, R.L. Scour effects on the response of laterally loaded piles considering stress history of sand. *Comput. Geotech.* **2010**, *37*, 1008–1014. [CrossRef]
25. Achmus, M.; Kuo, Y.S.; Abdel-Rahman, K. Numerical investigation of scour effect on lateral resistance of windfarm monopiles. In Proceedings of the 20th International Offshore and Polar Engineering Conference, Beijing, China, 20–25 June 2010; pp. 619–623.
26. Mostafa, Y.E. Effect of local and global scour on lateral response of single piles in different soil conditions. *Engineering* **2012**, *4*, 297–306. [CrossRef]
27. Li, F.; Han, J.; Lin, C. Effect of scour on the behavior of laterally loaded single piles in marine clay. *Mar. Georesour. Geotechnol.* **2013**, *31*, 271–289. [CrossRef]
28. Brinkgreve, R.; Kumarswam, S.; Swolfs, W. *Plaxis 3D Anniversary Edition Manual*; Plaxis bv.: Delft, The Netherlands, 2015.
29. Maghsoudloo, A.; Askarinejad, A.; Jager, R.R.D.; Molenkamp, F.; Hicks, M. Experimental investigation of pore pressure and acceleration development in static liquefaction induced failures in submerged slopes. In Proceedings of the 9th International Conference of Physical Modelling in Geotechnics, London, UK, 17–20 July 2018.
30. Roulund, A.; Sumer, B.M.; Fredsøe, J.; Michelsen, J. Numerical and experimental investigation of flow and scour around a circular pile. *J. Fluid Mech.* **2005**, *534*, 351–401. [CrossRef]
31. Hoffmans, G.J.; Verheij, H.J. *Scour Manual*; CRC Press: Boca Raton, FL, USA, 1997.
32. Schanz, T. Zur Modellierung des Mechanischen Verhaltens von Reibungsmaterialen. Ph.D. Thesis, Stuttgart University, Stuttgart, Germany, 1998. (In German).
33. Kondner, R.L. Hyperbolic stress-strain response: Cohesive soils. *ASCE J. Soil Mech. Found.* **1963**, *89*, 115–143. [CrossRef]
34. Duncan, J.M.; Chang, C.Y. Nonlinear analysis of stress and strain insoils. *ASCE J. Soil Mech. Found.* **1970**, *96*, 1629–1653. [CrossRef]
35. Brinkgreve, R.; Engin, E.; Engin, H.K. Validation of empirical formulas to derive model parameters for sands. In Proceedings of the 7th NUMGE 2010, Trodheim, Norway, 2–4 June 2010.

36. *JGS 0162-2009*; Tests for Physical Properties: Test Methods for Minimum and Maximum Densities of Sands. The Japanese Geotechnical Society: Tokyo, Japan, 2010; pp. 162–170.
37. Kishore, Y.N.; Rao, S.N.; Mani, J. Influence of the scour on laterally loaded piles. In Proceedings of the 12th International Conference of International Association for Computer Methods and Advances in Geomechanics, Goa, India, 1–6 October 2008; pp. 3283–3288.

Disclaimer/Publisher's Note: The statements, opinions and data contained in all publications are solely those of the individual author(s) and contributor(s) and not of MDPI and/or the editor(s). MDPI and/or the editor(s) disclaim responsibility for any injury to people or property resulting from any ideas, methods, instructions or products referred to in the content.